https://doi.org/10.5194/hess-2022-329
Preprint. Discussion started: 19 September 2022

Hydrology and Earth System Sciences
Open Access
Discussions

A tree-ring perspective on the past and future mass balance of a glacier in Tien Shan (Central Asia): an example from the Tuyuksu glacier, Kyrgyzstan

Youping Chen [1], Magdalena Opała-Owczarek [2], Feng Chen [1, 3*], Piotr Owczarek [4], Heli Zhang [3, 1], Shijie Wang [1], Mao Hu [1], Rysbek Satylkanov [5], Bakytbek Ermenbaev [5], Bakhtiyorov Zulfiyor [1, 6], Huaming Shang [3], Ruibo Zhang [3]

[1]Yunnan Key Laboratory of International Rivers and Transboundary Eco-Security, Institute of International Rivers and Eco-Security, Yunnan University, Kunming, 650500, China

[2]Institute of Earth Sciences, Faculty of Natural Sciences, University of Silesia in Katowice, Ul. Bedzinska 60, 41-200 Sosnowiec, Poland

[3]Key Laboratory of Tree-ring Physical and Chemical Research of the Chinese Meteorological Administration/Xinjiang Laboratory of Tree-ring Ecology, Institute of Desert Meteorology, Chinese Meteorological Administration, Urumqi, 830002, China

[4]Institute of Geography and Regional Development, University of Wroclaw, Pl. Uniwersytecki 1, 50-137 Wrocław, Poland

[5]Tien-Shan Mountain Scientific Center, Institute of Water Problems and Hydro Power, National Academy of Sciences of the Kyrgyz Republic, Bishkek, Kyrgyzstan;

[6]Khujand Science Center Academy of Sciences of the Republic of Tajikistan, Khujand, Tajikistan

Correspondence to: Feng Chen (feng653@163.com)

Abstract. The Tien Shan glaciers, known as "Central Asia's Water Tower," have a direct influence on water resource management in downstream parched areas. The limited time periods of currently available observational climate datasets hamper an accurate examination of glacial changes in Central Asia in terms of long-term climate change implications. In this work, we analysed this change by combining tree-ring-based reconstructions of the Tuyuksu Glacier's high-altitude mass balance during the last 382 years with models of the future mass balance of this glacier until the year 2100 CE. The results show that mountain precipitation is an important force driving the cycles of the cryosphere, biosphere and hydrosphere in arid Central Asia. This driving force has broad coherence in spatiotemporal variation, with periodic cycles and decadal shifts caused by the North Atlantic Oscillation and the El Niño-Southern Oscillation. The multi-model mean in CMIP6 suggests a downward trend in glacier mass balance until 2100, but this trend will be moderated by increased precipitation. The findings of the study could help to explain how the glacial mass balance has evolved in the Tien Shan Mountains of Central Asia throughout time and its relationship to other geosphere layers.

Keywords: Central Asia; Tuyuksu Glacier; mass balance reconstruction; Tree-ring; CMIP 6

1 Introduction

Numerous papers have reported rapid glacier melt worldwide resulting from ongoing global warming, the effects of which are particularly obvious in mountainous areas, especially in Central Asia, where temperatures have recently been at a high level (Xu et al., 2018; Zhang et al., 2019). Continuous glacier melt will have a significant impact on Central Asia's freshwater supplies, particularly in high-emission scenarios (Huss and Hock, 2018; Li et al., 2019; Li et al., 2020). The major Central Asian river basins of the Tarim, the Amu Darya and the Syr Darya will receive their maximum glacier meltwater input during the next few decades (Huss and Hock, 2018). This increases the likelihood of freshwater shortages and could lead to conflicts in fast-developing economies (Munia et al., 2016). The most direct evidence of a warming influence on glaciers is the glacier mass balance, which governs ice dynamics and glacier behaviour (Hagg et al., 2017; Azam et al., 2020; Liu et al., 2020; Shean et al., 2020). But because most glacier mass balance data from around the world are less than 50 years old, a comprehensive evaluation of glacier variations and responses to climate change on an inter-annual and decadal scale is impossible (Cerrato et al., 2020). Nevertheless, since glacier mass balance is largely influenced by climate, other proxies sensitive to the same factors can be used to reconstruct past mass balance series (Cerrato et al., 2020; Managave et al., 2020; Singh et al., 2021).

Tree rings are a valuable and sensitive proxy for recording past changes in glacial mass balance. In Asia, Singh (2021) employed a tree-ring isotope chronology from mixed conifers to reconstruct the fluctuation in glacial mass balance in the central Himalayas from 1743, finding that the loss of mass balance had accelerated since the 1960s. In Europe, Cerrato (2020) likewise employed tree-ring densities of Swiss stone pines to recreate the Careser Glacier's summer mass balance fluctuation. In previous research in Central Asia, tree rings were successfully applied to reconstruct precipitation, temperature and runoff variations in mountainous locations, but they were rarely employed to reconstruct glacial mass balance. Following the demise of the Soviet Union, a vast number of observations of huge glacier mass balances were halted. There have only ever been two long-term mass balance programmes: one at the Urumqi Glacier No. 1 in China and the other at the Tuyuksu Glacier in Kyrgyzstan. Such long-term observations are a good basis for understanding past changes in glacier mass balance based on tree rings.

https://doi.org/10.5194/hess-2022-329
Preprint. Discussion started: 19 September 2022

Few studies have hitherto utilized tree rings to analyse the Tuyuksu Glacier's mass balance, although it is worth noting that Zhang et al. (2019) employed annual ring isotopic chronology to estimate the Tuyuksu Glacier's mass balance variations from 1849 to 2014, finding that after 1968, melting was taking place without interruption and faster than at any time before.

We can achieve a better grasp of the variations in the Tuyuksu Glacier's mass balance on the basis of longer and more comprehensive data. In this study, we have sought (1) to explore the interplay between tree rings (biosphere) and glacial mass balance (cryosphere), precipitation and runoff (hydrosphere); (2) to undertake a reconstruction of the Tuyuksu Glacier's high-altitude mass balance variations between 1635 and 2016 CE based on tree-ring and mass balance responses, and to contrast the spatial and temporal characteristics of our reconstruction with other glacier balance masses and runoffs based on tree ring reconstruction; and (3) to look into the relationship with large-scale climatic forcings and predict how this will change in the future. The findings of this study will advance our knowledge of how climate change affects the mass balance of the Tuyuksu Glacier, as well as changes in tree growth and runoff around it, in the context of long-term scales.

2 Materials and methods

2.1 Geographical Settings

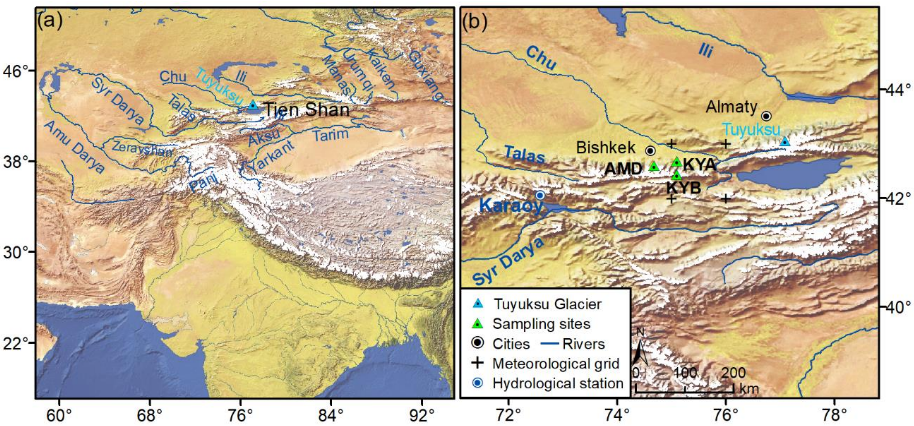

Figure 1: Distribution map of Tuyuksu Glacier and its surrounding main rivers in the Tien Shan Mountains of Central Asia (a). Location of tree-ring sampling sites, Karaoy hydrological station and CRU meteorological grid dataset around Tuyuksu Glacier (b).

Spanning most of Central Asia, with numerous glacial fluctuation sequences, the Tien Shan Mountains

https://doi.org/10.5194/hess-2022-329
Preprint. Discussion started: 19 September 2022

are considered to be the source of numerous permanent rivers, hence the appellation "Central Asia's Water Tower" given to them (figure1a). The Tuyuksu Glacier (77.08°E, 43.05°N) is situated in the Zailiyskiy Alatau Mountains in southern Kyrgyzstan, on the northern side of the Tien Shan Mountains, with an area of 2.3 km^2 (2013) and elevations ranging from 3478 to 4219 m a.s.l. The climate in the area is semi-arid continental affected by water-bearing westerly winds.

2.2 Tree-ring data

Picea schrenkiana and *Juniperus turkestanica* are the two main conifer species in the Tien Shan Mountains, usually distributed between 1800-3000 m a.s.l. We collected cores from them – two or three per tree using a 10 mm increment borer at breast height – (Codes KYA, KYB, and AMD) around the Tuyuksu Glacier in the summers of 2015 and 2016 (figure1b, table1). The forest stands chosen for sampling were only slightly affected by human agencies, if at all.

Table 1. Site information for the sampling sites.

Site	Lon. (E)	Lat. (N)	Elevation (m, a s l)	Aspect	Slope	Cores/Trees	Species
KYA	75.08°	42.49°	2600	E	20-30°	52/26	*Picea schrenkiana*
KYB	75.11°	42.56°	1990	E	20-30°	42/21	*Picea schrenkiana*
AMD	74.67°	42.6°	1830	E	30-40°	47/24	*Juniperus turkestanica*

The cores were mounted and polished in the laboratory using sandpaper (320, then 600 grains) using standard techniques. The tree rings were then examined visually, their widths measured, and cross-dated with an accuracy of 0.001 mm utilizing a Velmex measurement device. This enabled the calendar date of each ring to be given as the year in which the rings began to grow (Holmes, 1983). COFECHA software was used to do a statistical validation of the quality of cross-dating. The dendrochronological quality tests were passed by 141 ring-width series from a total of 71 trees.

Finally, all the individual series were normalized to eliminate biological growth patterns and the influence of non-climatic variables using ARSTAN software (Cook and Kairiukstis, 2013). Detrending was done using a negative exponential curve function for each series. To reduce the effects of outliers, all the individual detrended data were integrated into a regional chronology (RC) utilizing the biweight robust mean (Cook and Kairiukstis, 2013). The reliability of the chronology was examined using inter-series correlation (Rbar) and Expressed Population Signal (EPS; Wigley et al., 1984). Based on Rbar and sample depth, EPS $\geqslant$ 0.85 is the suggested threshold value for determining the robust elements of a

https://doi.org/10.5194/hess-2022-329
Preprint. Discussion started: 19 September 2022

Hydrology and Earth System Sciences
Discussions

chronology for reconstruction (Wigley et al., 1984). Based on the threshold values, the RC given below terminated before 1635 CE (figure 2).

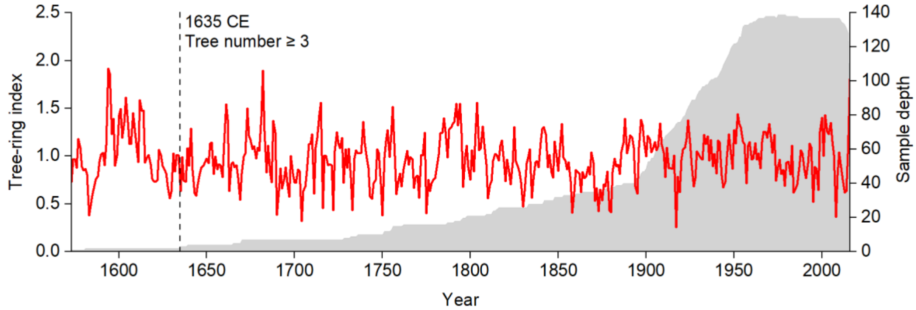

Figure 2: Regional chronology around the Tuyuksu Glacier in Central Asia over the period 1573-2016 and its sample depth. Vertical dashed line indicates the EPS threshold.

2.3 Glacier mass balance and meteorological data

We collected annual mass balance data for the Tuyuksu Glacier at 100 m altitude intervals between 3400-4200 m a.s.l. from 1969 to 2016 based on the World Glacier Monitoring Service (https://wgms.ch/) (figure 3a). Calculations show that fluctuations in the glacier mass balance at various elevations are quite constant (r_{mean} = 0.76). Meanwhile, as the altitude increases, so does the mass balance of the glacier. The future Tuyuksu Glacier mass balance simulation parameters were obtained from a 3-model (CanESM, CESM2, CESM2-WACCM, 33 ensemble members) ensemble mean of Phase 6 of the Coupled Model Intercomparison Project (CMIP6). This was done for both the 'historical' simulation period of 1850-2016 CE and the 'future' simulation period of 2017-2100 CE. Previous studies showed the selected multi-model to be more suitable for precipitation analysis in arid Central Asia than other Global Circulation Models in CMIP6 (Guo et al., 2021). We employed the low, medium and high typical concentration pathway scenarios (SSP126, SSP245, and SSP585, respectively) for the future simulation period. These simulation data were obtained from the KNMI-Climate Explorer (http://climexp.knmi.nl)

Based on the location information of the Tuyuksu Glacier, datasets of long-term gridded monthly mean temperature and monthly total precipitation were obtained from the Climatic Research Unit (CRU TS 4.05, 0.5° latitude × 0.5° longitude, 42°-43°N, 75°-76°E, 1969-2016; Harris et al., 2020). According to meteorological statistics, the average annual precipitation is 359.8 mm, with the wet summer months (April-September) receiving around 59% of the annual total. The average annual temperature varies by around 2.2 ℃, with a minimum of -14.0 ℃ in January and a maximum of 15.6 ℃ in July (figure 3b).

https://doi.org/10.5194/hess-2022-329
Preprint. Discussion started: 19 September 2022

This weather information also came from the KNMI-Climate Explorer. (http://climexp.knmi.nl). Since certain impacts of teleconnection patterns on the Tuyuksu Glacier's mass balance have already been published (Zhang et al., 2019), we further looked at the linkages between the North Atlantic Oscillation (NAO; Trouet et al., 2009) and the El Niño-Southern Oscillation (ENSO; Li et al., 2011) to see how teleconnection patterns affect the region's glacier mass balance in the context of long time scales.

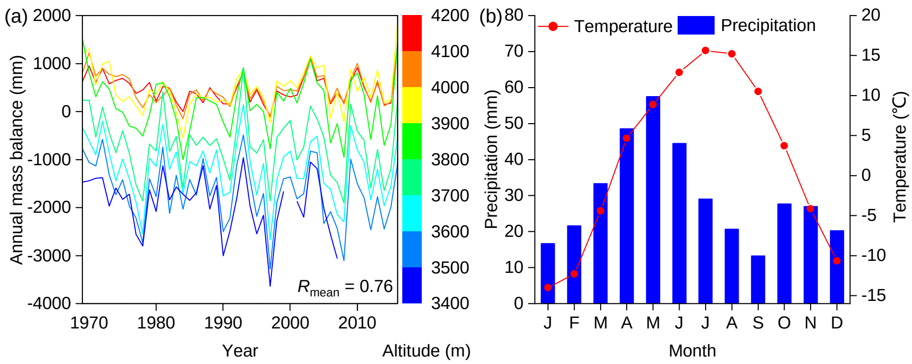

Figure 3: Time series of gauged annual mass balance at different gradients of the Tuyuksu Glacier (1969-2016) (a). Monthly total precipitation and mean temperature from the CRU TS 4.05 (1969-2016) (b).

2.4 Statistical methods

Pearson correlation analyses were carried out on the tree-ring data with glacial mass balance records and meteorological data. Correlations between the altitude combination of glacier mass balance and tree-ring series were also investigated in order to choose the best altitude for reconstructing the glacier mass balance.

Then, based on the correlation analysis, a linear regression model was employed to reconstruct the variation in the Tuyuksu Glacier's mass balance. Owing to the limited record of experimental glacier mass balances, the leave-one-out cross-validation approach (Michaelsen, 1987) was taken to assess the model's prediction potential. The correlation coefficient (r), explained variance (r^2), reduction of error (RE), product of means test (PMT) and sign test (ST) were all employed as test values. Using 31-year low-pass values, we identified periods of positive and negative mass balance for the reconstruction, where the reconstructed periods were constantly higher or lower than the long-term reconstructed average from 1635 to 2016 for more than 10 years.

Finally, to see whether our glacier mass balance reconstructions had any links to large-scale atmospheric circulations, we used the multitaper spectral (Mann and Lees, 1996) to evaluate the frequency domain properties of the reconstructed series. Moreover, the Pearson correlation was used again to indicate the relationships of Oscillation Periods between the reconstructed sequence and the NAO and ENSO, extracted on the basis of singular spectrum analysis (Vautard, 1992). Meanwhile, to probe the teleconnections of glacier mass balance to oceans, we created two composite sea surface temperature anomaly maps based on the gridded sea surface temperature dataset (Smith and Reynolds, 2003) for the 10 highest and the 10 lowest glacier mass balance years from 1969 to 2016 in order to illustrate the different spatial patterns of sea surface temperatures.

3 Results

3.1 Glacier mass balance – tree-ring growth response

The results of the correlation analysis are shown in figure 4. The RC was significant positively correlated with the annual glacier mass balance at altitudes of 3500-3600 (r = 0.47, p < 0.01), 3600-3700 (r = 0.45, p < 0.01), 3700-3800 (r = 0.52, p < 0.01), 3800-3900 (r = 0.61, p < 0.01), 3900-4000 (r = 0.62, p < 0.01), 4000-4100 (r = 0.58, p < 0.01) and 4100-4200 m (r = 0.51, p < 0.01), while the correlation declined at 3400-3500 m a.s.l. (r = 0.29) (figure 4a). With a wide range of altitude combinations, the strongest correlations were found between the RC and the annual glacier mass balance variability at high altitudes from 3800 to 4100 m a.s.l. ($GMB_{3800\text{-}4100}$; r = 0.634, p < 0.01; figure 4a). The radial growth response to glacier mass balance was better at higher than at lower altitudes.

Both tree radial growth and glacier mass balance are aided by precipitation. We began by investigating the connection between precipitation and glacier mass balance. Figure 4b shows that there were substantial positive associations between precipitation and the $GMB_{3800\text{-}4100}$ in April (r = 0.47, p < 0.01), May (r = 0.30, p < 0.05), June (r = 0.38, p < 0.01), July (r = 0.51, p < 0.01) and August (r = 0.37, p < 0.05) during 1969-2016. Moreover, the April-September precipitation had the strongest significant positive connection with $GMB_{3800\text{-}4100}$ (r = 0.675; p < 0.01). In contrast, $GMB_{3800\text{-}4100}$ showed substantial negative relationships with mean monthly temperatures in May (r = -0.30; p < 0.05), July (r = -0.50; p < 0.01) and August (r = -0.36; p < 0.05). The strongest negative associations between $GMB_{3800\text{-}4100}$ and mean monthly temperatures were found for July-August (r = -0.532; p < 0.01). Overall, our findings indicate that fluctuations in the Tuyuksu Glacier's high-altitude mass balance are predominantly controlled by precipitation.

It can also be seen from figure 4c that there was a significant correlation between the RC and mean temperature in January (r = 0.34, p < 0.05) and July (r = -0.31, p < 0.05), as well as the precipitation in the previous July (r = 0.30, p < 0.05), August (r = 0.36, p < 0.05) and October (r = 0.29, p < 0.05) and the current April (r = 0.41, p < 0.01), May (r = 0.44, p < 0.01) and July (r = 0.42, p < 0.01). The largest association between the RC and average temperature came from the previous December-February (r = 0.47, p < 0.01), whereas the best correlation with precipitation came from the previous July-June (r = 0.67, p < 0.01). Based upon the above results, it appears that precipitation during recent and previous growing seasons accounts for the majority of climatic factors affecting the radial growth of trees.

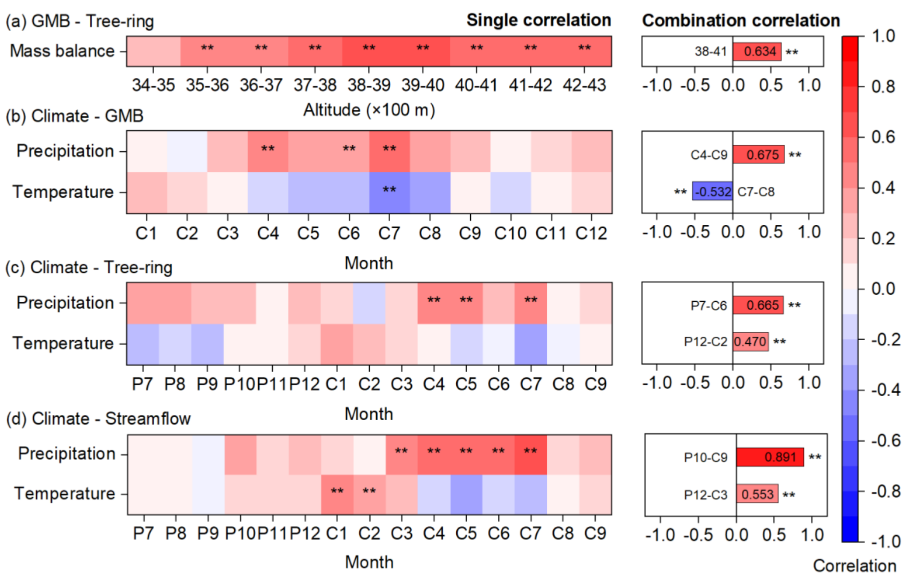

Figure 4: Correlations of regional chronology with annual mass balance of the Tuyuksu Glacier at different gradients (a). Correlations between monthly precipitation and mean temperature from the CRU TS4.05 with the glacial annual mass balance at 3800-4100 m a.s.l (b), regional chronology (c) and annual runoff of Talas River (d). "P", "C" and "" represent previous year, current year and 99% significant correlation, respectively.**

3.2 Annual glacier mass balance reconstruction

In accordance with the findings of the interplay between tree-ring development and the annual mass balance of the Tuyuksu glacier at 3800-4100 m a.s.l., we recreated a linear regression model as follows: $GMB_{3800\text{-}4100}$ = 997.208 RC - 586.915 (1969-2016, r = 0.634, r^2 = 40.3%, F = 30.99, and p < 0.0001)(figure 5a). Comparison of the reconstructed and observed $GMB_{3800\text{-}4100}$ series from 1969 to 2016 indicated that the model fit was typically good (figure 5b). The leave-one-out cross-validation procedure

https://doi.org/10.5194/hess-2022-329
Preprint. Discussion started: 19 September 2022

Hydrology and Earth System Sciences
Discussions

demonstrated that the regression model was resilient and dependable over time, and statistics validated the reconstruction. The positive result of RE (0.34) verified the regression model's validity. Meanwhile, the PMT (4.598, $p < 0.05$) and ST (32+, 16-, $p < 0.05$) statistics were significant, showing that the real and calculated values for high-frequency fluctuations were generally consistent. It was therefore feasible to reconstruct the $GMB_{3800\text{-}4100}$ over the past 382 years using the above linear regression model (figure 5c).

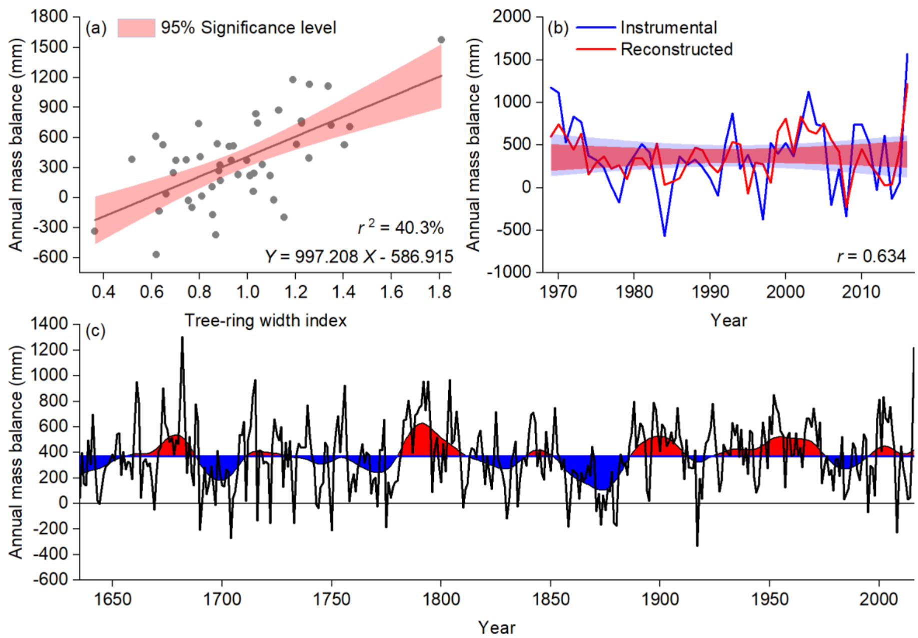

Figure 5: Scatter plot of regional chronology and annual mass balance at 3800-4100 m a.s.l of the Tuyuksu Glacier with linear fitting curve for the common period 1969-2016 (a). Comparison between the instrumental and reconstructed annual mass balance of the Tuyuksu Glacier (b). Reconstructed annual mass balance at 3800-4100 m a.s.l of the Tuyuksu Glacier since 1635 (black line). The blue and red shaded area show the data smoothed with a 31-year low-pass filter to emphasise the long-term fluctuations (c).

3.3 Characteristics of the glacier mass balance reconstruction

The $GMB_{3800\text{-}4100}$ reconstruction and 31-year low-pass filtered data for the Tuyuksu Glacier in the Tien Shan Mountains of Central Asia are illustrated in figure 5c. For the period 1635-2016, the $GMB_{3800\text{-}4100}$ reconstruction comprised a significant number of high and low frequencies. The long-term average and standard deviation of the reconstructed $GMB_{3800\text{-}4100}$ were 369.9 mm and 253.0 mm, with the maximum and minimum amounts occurring in 1682 (1305.8 mm) and 1917 (-334.6 mm). We also found multiple ten-year or longer positive and negative periods. Positive spells were found for the periods 1656-1687,

https://doi.org/10.5194/hess-2022-329
Preprint. Discussion started: 19 September 2022

1712-1730, 1780-1811, 1839-1851, 1887-1912, 1924-1975 and 1996-present, whereas the periods 1635-1655, 1688-1711, 1731-1779, 1812-1838, 1852-1886, 1913-1923 and 1976-1995 were all shown to be negative. Interestingly, the reconstruction series did not indicate a significant ablation trend during the current warming phase.

Figure 6a shows the multi-decadal cycle of 48.5 years detected in the reconstructed $GMB_{3800\text{-}4100}$ sequence using MTM analysis. Meanwhile, some other inter-annual cycles were also discovered with the following periods: 5.3 years (99%), 4.1-4.3 years (95%), 3.3-3.6 years (95%), 2.9 years (99%), 2.7 years (95%), 2.3 years (99%) and 2.1 years (99%). This suggests that changes in the $GMB_{3800\text{-}4100}$ are likely to be closely tied to large-scale ocean-atmosphere-land circulations. We further extracted the periodic oscillations of $GMB_{3800\text{-}4100}$, NAO and ENSO, based on the SSA method. Correlation analysis showed that $GMB_{3800\text{-}4100}$ was highly negatively correlated with the NAO on a 48.5-year cycle scale (r = -0.58, p < 0.01) and positively correlated with the ENSO on a 5.3-year cycle scale (r = 0.26, p < 0.01) (figure 6b). Likewise, composite maps of the ten highest (figure 6c) and lowest $GMB_{3800\text{-}4100}$ (figure 6d) years demonstrated that excessively positive and negative $GMB_{3800\text{-}4100}$ corresponds to NAO and ENSO occurrences. According to the results of this research, NAO and ENSO are the primary processes responsible for high-altitude mass balance shifts in the Tuyuksu Glacier.

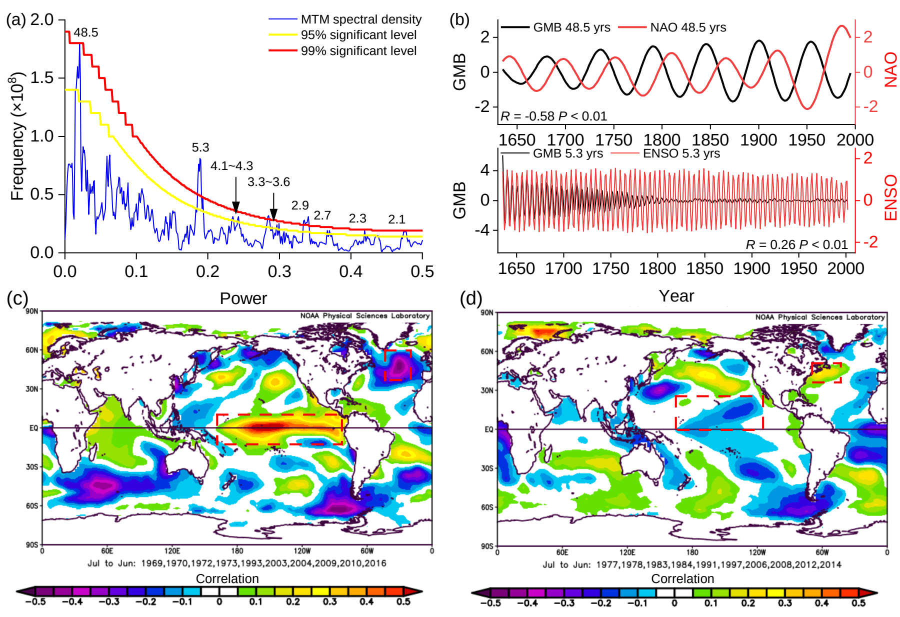

Figure 6: Spectral signal of the glacier mass balance reconstruction from 1635 to 2016, with blue and red lines indicating the 95% and 99% confidence limits (a). Comparison of low frequency signals of the reconstructed

https://doi.org/10.5194/hess-2022-329
Preprint. Discussion started: 19 September 2022

glacier mass balance and ENSO, NAO based on singular spectrum analysis (b). Composite maps of SST for the 10 highest glacier mass balance (c) and 10 lowest glacier mass balance (d) years.

4 Discussion

4.1 Glacier mass balance, tree-ring, runoff and climate

Mountain glaciers are extremely susceptible to changes in temperature and precipitation, particularly in arid regions like Central Asia. The key influencing element for the fluctuation of mass balance at the high altitude of the Tuyuksu Glacier is precipitation from April to September. The fundamental causes of glacial oscillations are temperature, precipitation and regional climatic inputs (Zhang et al., 2019). Greater snowfalls or lower temperatures promote positive mass balances, causing glaciers to expand. Conversely, glaciers retreat when precipitation is insufficient or temperatures are too high. The precipitation from April to September accounts for 59% of the annual amount, which contributes to the build-up of the mass balance of high-altitude glaciers. As a result, the mass balance variation at the Tuyuksu Glacier's high elevations must be affected by precipitation from April to September. A similar level of precipitation in the high-altitude response of snow mass was also reported by Yang (2021) in the Tien Shan Mountains. Likewise, recent research has discovered that precipitation plays a significant role in the mass balance of the Naimona'nyi glacier on the northern Himalayan slopes (Zhu et al., 2021).

On the other hand, during the pre-growing and growing seasons, precipitation has a significant positive influence on the radial development of *Picea schrenkiana* and *Juniperus turkestanica*, with a greater impact during the active growing season. Firstly, physiologically, with an average temperature of 13.8 °C and a total annual precipitation of 62.0 mm (figure 3b), the time between the previous July and September represents the middle to the end of the study area's tree growing season. Larger leaves grow as a result of this circumstance, which also encourages the build-up of photosynthetic materials in trees (Liu et al., 2011). This expands the total photosynthetic and absorptive areas of trees, enabling them to photosynthesize or absorb precipitation the next year when favourable climatic conditions prevail (Fritts, 1976). Secondly, the previous October-April period was the non-growing season for trees, with a mean temperature of -5.3°C and 193.7 mm of total precipitation (figure 3b). Sufficient snowfall during this period allowed trees to absorb more water in the early growth season (Díaz et al., 2002). Finally, the current May-June was the key season for tree growth, with an average temperature of 10.9 °C and a total precipitation of 101.9 mm (figure 3b). Rainfall increased during this time, which increased soil moisture

https://doi.org/10.5194/hess-2022-329
Preprint. Discussion started: 19 September 2022

and further encouraged the production of cambium cells (Liu et al., 2011). Similar climate responses for the tree species in this study were also reported in northern Kyrgyzstan (Zhang et al., 2019), southern Kazakhstan (Zhang et al., 2017) and the Ili-Balkhash basin (Chen et al., 2017) in Central Asia and were in agreement with studies on *Larix sibirica* in the Tien Shan Mountains of Central Asia (Chen et al., 2015).

Importantly, $GMB_{3800\text{-}4100}$ has no direct effect on the radial growth of trees on mountain slopes. Nevertheless, they are both impacted by the same precipitation forcing, with a correlation value of 0.72 between April-September and the previous July-June precipitation from 1969 to 2016. It is reasonable to infer that the development of trees in the research region is a good indicator of the variability of glacial mass balance at high altitudes. As changes in runoff in this area may also depend on precipitation, we selected the instrumental runoff from the Karaoy hydrological station of the Talas River near the Tuyuksu Glacier (figure 1b) for further response analysis (figure 4d). The results showed that the annual runoff was significantly positively correlated with the average temperature in January (r = 0.40, p < 0.01) and February (r = 0.40, p < 0.01), and with the precipitation in March (r = 0.41, p < 0.01), April (r = 0.55, p < 0.01), May (r = 0.52, p < 0.01), June (r = 0.56, p < 0.01) and July (r = 0.62, p < 0.01). The strongest correlation between annual runoff and mean temperature was from December to March (r = 0.553, p < 0.01), while the best correlation with precipitation occurred from October to September (r = 0.891, p < 0.01). Therefore, the change of runoff in this area is also mainly affected by precipitation. In summary, we can conclude that mountain precipitation in arid regions is the main driving force for the cryosphere (glacier mass balance), biosphere (tree-ring) and hydrosphere (runoff) (figure 7).

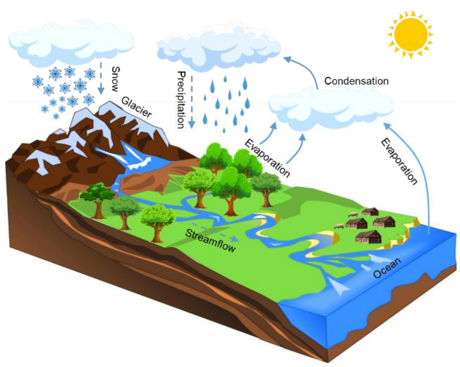

Figure 7: A conceptual model of the hydrological cycle between layers of the Earth's sphere, including the cryosphere, biosphere, and hydrosphere.

https://doi.org/10.5194/hess-2022-329
Preprint. Discussion started: 19 September 2022

4.2 Spatial representativeness

Since precipitation has a strong link with RC and $GMB_{3800-4100}$, we used the corresponding timeframe to investigate the spatial correlation of RC and $GMB_{3800-4100}$ with gridded precipitation from 1969 to 2016. A significant correlation field ($r > 0.5$) encompassing eastern Kyrgyzstan and south-eastern Kazakhstan was discovered by spatial correlation analysis (figure 8). This shows that our reconstruction incorporates $GMB_{3800-4100}$ variability in a large geographical range, particularly the Tuyuksu glacier area.

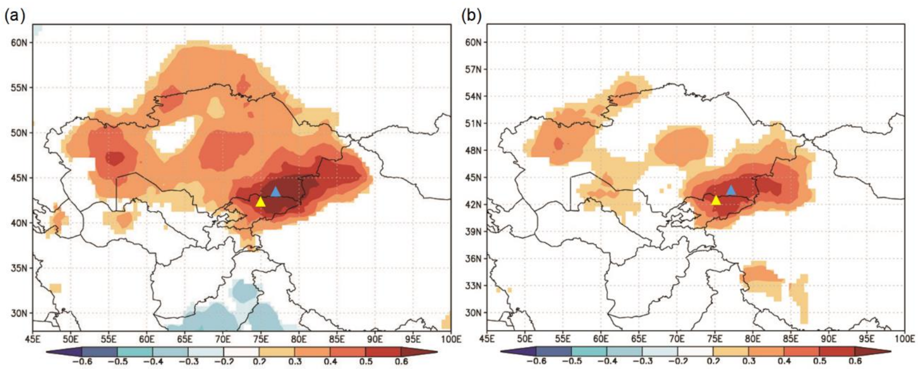

Figure 8: Spatial correlation pattern between reconstructed glacier mass balance and gridded July-June (a) and April-September (b) precipitation over the common period of 1969-2016. The yellow and blue triangles represent the sampling point and the location of the Tuyuksu Glacier.

Further, we contrasted our reconstruction (figure 9a) with the earlier sequence of reconstructions of this glacier's mass balance made by Zhang et al. (2019) (figure 9b). The results of the comparison showed that the two reconstructed sequences were matched to a high degree (r = 0.60, p < 0.01, 1850-2015). Notably, positive glacial mass balance periods occurred during 1888-1910, 1924-1942 and 1949-1973, whereas the periods 1857-1887, 1913-1923 and 1976-1995 were relatively negative. These consistent findings confirm our model of glacial mass balance. However, we also note that the difference between the two series is that our reconstructed series shows no negative trend in the context of global warming since 1996. The reason may be that the cold temperatures and greater snowfall at high altitudes offset the melting effect of temperature on the ice and snow (Yang et al., 2021). We extended the reconstruction value of this glacier's mass balance sequence back to 1635, which is 216 years longer.

We also compared our reconstructed series with those of other northern hemisphere glaciers. In Asia, positive glacier mass balance periods from 1780-1811 and 1839-1851, and negative glacier mass balance periods from 1976-1995, were consistent with the glacial mass balance of the central Himalayas reconstructed by Singh et al. (2021) based on ice cores and tree rings, and the positive mass balance of the Hailuogou Glacier on the Tibetan Plateau in the 1960s was also reflected in our reconstruction sequence (Duan et al., 2013). In North America, the mass balance reconstruction sequence of the Place Glacier in British Columbia, compared with our sequence, was simultaneously positive during 1656-1687, 1800-1811 and 1960-1975, and simultaneously negative during 1852-1865 (Wood et al., 2011). Likewise, both the Peyto Glacier in Canada and our glacier reconstruction sequence were negative for the period 1760-1779 (Watson et al., 2004). The negative mass balance of the South Cascade Glacier over the period 1790-1800 reported by Marcinkowski et al. (2012) also appeared in our reconstruction sequence. In Europe, high-resolution reconstructions of the Storglaciären mass balance in northern Scandinavia based on tree-ring data and circulation indices co-varied with our sequence during 1890-1910 and the mid-1820s-early 1830s (Linderholm et al., 2007). Similarly, in the Polar Ural, the positive glacier mass balance during the 1930s-1940s and the negative glacier mass balance during 1913-1923 and 1987-2000 in our series were also reflected in the Ural glacier (Kononov et al., 2005). The foregoing comparison reveals that the mass balances of the Tuyuksu glacier and Northern Hemisphere glaciers have a synergistic shift in space and time. Furthermore, the comparative results corroborate the accuracy of the Tuyuksu Glacier's mass balance reconstruction.

Both runoff and glacier mass balance are affected by precipitation. We compared the reconstructed $GMB_{3800-4100}$ (figure 9a) with the surrounding river runoff sequence based on tree-ring reconstruction, such as the Chu River (Gao et al., 2022, figure 9c), the Manas River (Yuan et al., 2007, figure 9d), the Urumqi River (Yuan et al., 2013, figure 9e), the Kaiken River (Zhang et al., 2020, figure 9f) and the Guxiang River (Chen et al., 2016, figure 9g). After truncating the runoff reconstructions of these rivers before 1635 CE, all runoff reconstructions were smoothed with a 31-year low-pass filter and scaled to zero to emphasize low-frequency changes in runoff. The reconstructed $GMB_{3800-4100}$ had the best correlation with the runoff sequence of the Chu River, with a correlation coefficient of 0.60 ($p < 0.01$), and was also significantly positively correlated with the reconstructed runoff of the Urumqi River ($r = 0.16$, $p < 0.01$), the Manas ($r = 0.15$, $p < 0.01$), the Kaiken ($r = 0.20$, $p < 0.01$) and the Guxiang ($r = 0.18$, $p < 0.01$). According to the majority of data, positive periods dominated in 1675-1687, 1782-1794, 1889-1905, 1932-1942 and 1949-1973, whereas negative periods prevailed in 1812-1829, 1857-1871, 1913-1923 and 1978-1992. In conclusion, the consistency of the positive and negative periods of these curves on the inter-decadal scale suggests that the precipitation-influenced changes to the cryosphere, biosphere

https://doi.org/10.5194/hess-2022-329
Preprint. Discussion started: 19 September 2022

Hydrology and Earth System Sciences
Discussions

and hydrosphere in the Tien Shan Mountains of Central Asia are generally characterized by a similar large-scale spatiotemporal variability.

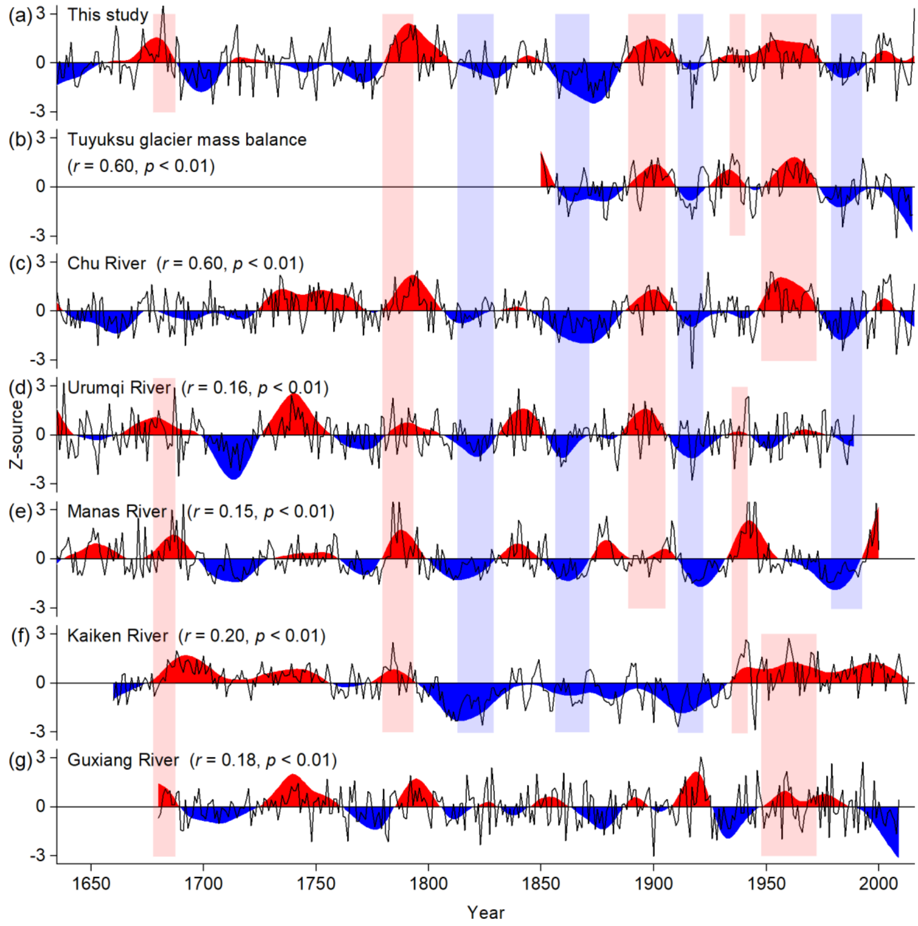

Figure 9: Comparison between the glacier mass balance reconstructed in this study (a) and the glacier mass balance reconstructed by Zhang et al. 2019 (b). and the reconstructed runoff of the Chu River (c), Urumqi River (d), Manas River (e), Kaiken River (f) and Guxiang River (g). The series were smoothed with a 31-year moving average to emphasize long-term fluctuations and the shadow means the common high/low periods.

4.3 Large-scale climate forcings

A substantial inverse relationship between the $GMB_{3800\text{-}4100}$ reconstruction and the NAO was discovered, demonstrating that atmospheric circulation in the North Atlantic influenced hydroclimatic variability in Central Asia. Previous research revealed that the NAO anomaly influenced water vapour transfer from Iceland to Scandinavia and then to the Tien Shan Mountains via cyclone activity, hence modifying the subtropical westerly jet in Asia. The Tien Shan Mountains exhibit anticyclonic circulation during positive

https://doi.org/10.5194/hess-2022-329
Preprint. Discussion started: 19 September 2022

NAO phase years, when the westerly wind component is reduced and the water vapour content drops; the converse holds true during negative NAO episodes (Hao et al., 2022). A similar association was documented for the reaction to climate change on the Urumqi No. 1 glacier in the Tien Shan Mountains, demonstrating that this forcing has an impact on various Central Asian locations (Hao et al., 2022). Lan et al. (2018) reconstructed the climate changes in the central South Tien Shan over the past two millennia based on glacial lake sediment cores, and the reconstruction results were verified by records such as lake sediments, stalagmites, ice cores and tree rings, indicating that Central Asian Climate patterns have been closely linked to the phases of the NAO during the past two thousand years. Recent research has demonstrated that the significant remnants of the Laurentide and Fennoscandian ice sheets have an impact on this pattern (Lan et al., 2021). Our findings demonstrated a strong positive correlation between regional precipitation variability and the high-altitude mass balance of the Tuyuksu Glacier. Therefore, it is not unexpected that the history of our high-altitude mass balance reconstruction exhibits the signature of NAO occurrences.

Our findings also revealed a strong positive correlation between ENSO and $GMB_{3800\text{-}4100}$, suggesting that changes in the eastern Pacific's atmospheric circulation could be another source of $GMB_{3800\text{-}4100}$ forcing, in addition to the NAO. Other Central Asian regions also showed an association between water vapour variability and ENSO (Chen et al., 2021), i.e. the Kuramin Range (Northern Tajikistan) (Chen et al., 2019), the Altai Mountains (Kang et al., 2021), the Kuramenian Mountains (Republic of Tajikistan) (Chen et al., 2018), the Ili-Balkhash Basin (Chen et al., 2017), the western Tien Shan Mountains (Zhang et al., 2015), the Dzungarian Alatau (Zhang et al., 2017) and the Kara Darya River (Zhang et al., 2020). During warm ENSO phases, the unusually high south-westerly moisture flow brings abundant moisture over the Iranian Plateau and northwards, leading to improved precipitation across Central Asia, which is beneficial for tree development and the formation of the Central Asian glacial mass balance. The opposite pattern is produced during ENSO periods with cold temperatures (Mariotti, 2007). Furthermore, ENSO influences the mass balance of glaciers in other regions of the Northern Hemisphere, such as British Columbia's southern Coast Mountains (Larocque et al., 2005), the Western Himalayas (Shekhar et al., 2017) and the tropical Andes (Jonaitis et al., 2021).

4.4 Prediction of future glacier mass balances

Since mountain precipitation is the main driving force for the various geosphere layers (including the

https://doi.org/10.5194/hess-2022-329
Preprint. Discussion started: 19 September 2022

cryosphere) in Central Asia, we further derived projections of future Tuyuksu Glacier mass balances from climate model simulations participating in the sixth phase of the CMIP6 under the SSP126, SSP245 and SSP585 scenarios, respectively. First, based on the significant relationship between the observed glacier mass balance at high altitude ($GMB_{3800\text{-}4100}$) and precipitation from April to September ($P_{4\text{-}9}$), we created the following linear model: $GMB_{3800\text{-}4100} = 5.6325\ P_{4\text{-}9} - 825.22$ (1969-2016, $r = 0.675$, $r^2 = 45.5\%$, $F = 38.44$, and $p < 0.0001$). Then, we selected the simulated precipitation from April to September in the multi-model mean of CMIP6 under the above three scenarios and applied them to this linear model to generate mass balance forecasts for the Tuyuksu Glacier with continuous simulations from 1850 to 2100. The future multi-model ensemble glacier mass balance forecast indicates that the mass balance generally shows an increasing trend from 2017 to 2100 under different scenario models. The multi-year averages in the SSP126, SSP245 and SSP585 scenarios are about 134 mm, 135 mm and 129 mm higher than the averages of the reconstruction series from 1850 to 2016, respectively, accounting for about 36% (figure 10a). This increasing trend is also evident when contrasting the probability density function of the instrumental data between 1969 and 2016 CE and the entire reconstruction period between 1635 and 2016 CE with the probability density function of the ensemble members of the CMIP6 SSP126, SSP245 and SSP 585 scenario glacier mass balance projections between 2016 and 2100 CE (figure 10b).

However, we also noticed that the high-altitude mass balance of Tuyuksu Glacier ($GMB_{3800\text{-}4100}$) was significantly negatively correlated with the average temperature in July-August ($T_{7\text{-}8}$). Therefore, in the context of global warming, in order to accurately assess the impact of temperature rise on the glacier mass balance in this region, we first created the following linear model: $GMB_{3800\text{-}4100} = -310.33\ T_{7\text{-}8} + 5162.5$ (1969-2016, $r = 0.532$, $r^2 = 28.3\%$, $F = 18.14$, and $p < 0.0001$). Then, we screened the simulated mean temperature from July to August under the SSP126, SSP245 and SSP858 scenarios in the multi-model, and finally applied this linear model to calculate the mass balance of the glacier that is affected only by temperature. Comparison of the glacier mass balance series affected only by precipitation and temperature leads to the conclusion that a strong temperature increase causes the glacier mass balance to decline in general, whereas increased precipitation mitigates this process (figure 10c-e). The glacial mass balance ablation caused by precipitation relieving temperatures was approximately 66 mm, 174 mm and 213 mm, delayed by 16, 15 and 7 years under different scenarios.

https://doi.org/10.5194/hess-2022-329
Preprint. Discussion started: 19 September 2022

Hydrology and Earth System Sciences
Discussions

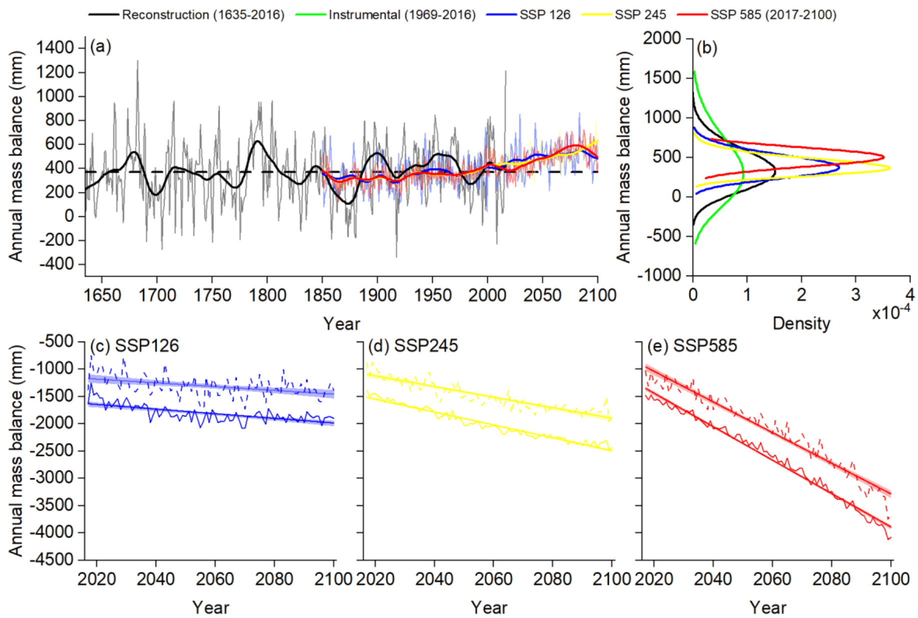

Figure 10: Reconstructed annual Tuyuksu Glacier mass balances from 1635 to 2016 and precipitation-derived glacier mass balances based on multi-model ensembles under the SSP126, SSP245 and SSP585 scenarios. The thick and dashed lines represent the 31-year low-pass filtered curve and the multi-year average (a). Probability density estimates for the multimodal simulated glacier mass balance for three periods: the instrumental (1969-2016), historical (1850-2016), and future SSP126, SSP245, and SSP585 (2017-2100), showing an increased trend of the positive annual mass balance under future high greenhouse gas emission scenarios (b). Comparison of the glacier mass balance series derived from temperature simulations (solid line) and the difference between the glacier mass balance series derived from precipitation simulations (dashed line) under different scenarios (c-e).

5 Conclusion

Based on fresh and regional tree-ring width chronologies collected from 141 *Picea schrenkiana* and *Juniperus turkestanica* trees growing in water-stressed parts of Central Asia's Tien Shan Mountains, we found a substantial link between tree growth and the Tuyuksu Glacier's high-altitude mass balance. Further response analysis showed that mountain precipitation was the most important driving force in the cryosphere, biosphere and hydrosphere in the study area. At the same time, this very close link enabled us to reconstruct this mass balance from 1635 to 2016 CE, the longest mass balance record obtained for the Tuyuksu Glacier to date. Over the last 382 years, the reconstruction indicated periods of positive and negative mass balance. The reconstructed history revealed that the mass balance of glaciers at high elevations has lately remained steady, which contradicts the overall mass balance breakdown.

https://doi.org/10.5194/hess-2022-329
Preprint. Discussion started: 19 September 2022

Furthermore, over the last 382 years, the reconstruction sequence has shifted on a decadal scale in tandem with other Northern Hemisphere glacial mass balances and Tien Shan runoff based on tree-ring reconstructions. We observed that large-scale atmospheric circulation influences a major part of the reconstructed glacier mass balance changes (NAO, ENSO). Thus, our findings point to intricate relationships between climatic variables from the tropical Pacific and North Atlantic. Finally, climate model simulations in CMIP6 suggest that increased precipitation will delay the impact of sharply rising temperatures on glacier mass balance ablation by 16, 15 and 7 years under the SSP126, SSP245 and SSP585 scenarios, respectively. This new mass balance record and further analysis add to our understanding of the Tuyuksu Glacier's long-term variability.

Data availability. Data set available on request to corresponding authors.

Author contributions. Conceptualization: Feng Chen, Youping Chen, Rysbek Satylkanov. Data curation: Feng Chen, Heli Zhang, Huaming Shang, Ruibo Zhang. Formal analysis: Feng Chen, Youping Chen, Shijie Wang, Mao Hu. Funding acquisition: Feng Chen. Investigation: Feng Chen, Youping Chen, Heli Zhang, Huaming Shang, Ruibo Zhang, Rysbek Satylkanov, Bakytbek Ermenbaev, Bakhtiyorov Zulfiyor. Methodology/ Project administration/ Resources: Feng Chen. Software: Feng Chen, Youping Chen. Supervision: Feng Chen. Validation: Youping Chen. Visualization/ Writing-original draft preparation/ Writing-review & editing: Feng Chen, Youping Chen, Magdalena Opała-Owczarek, Piotr Owczarek.

Competing interests. The authors declare that they have no known competing financial interests or personal relationships that could have influenced the work reported in this paper.

Acknowledgements. This research was supported by NSFC (U1803341 and 32061123008) and the National Key R&D Program of China (2018YFA0606401). We are very grateful to the reviewers, whose comments have greatly helped to improve this manuscript.

References

Azam, M. F. and Srivastava, S.: Mass balance and runoff modelling of partially debris-covered Dokriani Glacier in monsoon-dominated Himalaya using ERA5 data since 1979, J. Hydrol., 590, https://doi.org/10.1016/j.jhydrol.2020.125432, 2020.

Cerrato, R., Salvatore, M. C., Gunnarson, B. E., Linderholm, H. W., Carturan, L., Brunetti, M., and

Baroni, C.: *Pinus cembra L.* tree-ring data as a proxy for summer mass-balance variability of the Careser Glacier (Italian Rhaetian Alps), J. Glaciol., 66, 714-726, https://doi.org/10.1017/jog.2020.40, 2020.

Chen, F., Yu, S. L., Shang, H. M., Zhang, R. B., Zhang, T. W., Zhang, H. L., Chen, Y. P., Satylkanov, R., Ermenbaev, B., Kobuliev, Z., Ahmadov, A., Kodirov, A., and Maisupova, B.: The Productivity of Low-Elevation Juniper Forests in Central Asia Increased Under Moderate Warming Scenarios, J. Geophys. Res-Biogeo., 126, https://doi.org/10.1029/2021JG006269, 2021.

Chen, F. and Yuan, Y. J.: Streamflow reconstruction for the Guxiang River, eastern Tien Shan (China): linkages to the surrounding rivers of Central Asia, Environ Earth Sci, 75, https://doi.org/10.1007/s12665-016-5849-1, 2016.

Chen, F., Yuan, Y. J, and Yu, S. L: Tree-ring indicators of rainfall and streamflow for the Ili-Balkhash Basin, Central Asia since CE 1560, Palaeogeogr. Palaeocl., 482, 48-56, https://doi.org/10.1016/j.palaeo.2017.05.029, 2017.

Chen, F., Yuan, Y. J, Yu, S. L, Zhang, T.W, Shang, H. M, Zhang, R. B., Qin, L., and Fan, Z. A: A 225-year long drought reconstruction for east Xinjiang based on Siberia larch (*Larix sibirica*) tree-ring widths: Reveals the recent dry trend of the eastern end of Tien Shan, Quatern Int., https://doi.org/10.1016/j.quaint.2014.11.055, 358, 42-47, 2015.

Chen, F., Zhang, T. W., Seim, A., Yu, S. L, Zhang, R. B., Linderholm, H. W., Kobuliev, Z. V., Ahmadov, A., and Kodirov, A.: Juniper tree-ring data from the Kuramenian Mountains (Republic of Tajikistan), reveals changing summer drought signals in western Central Asia, Clim. Past. Discuss., 1-27, https://doi.org/10.5194/cp-2018-44, 2018.

Chen, F., Zhang, T. W., Seim, A., Yu, S. L., Zhang, R. B., Linderholm, H. W., Kobuliev, Z. V., Ahmadov, A., and Kodirov, A.: Juniper Tree-Ring Data from the Kuramin Range (Northern Tajikistan) Reveals Changing Summer Drought Signals in Western Central Asia, Forests., 10, 505, https://doi.org/10.3390/f10060505, 2019.

Cook, E. R. and Kairiukstis, L. A.: Methods of dendrochronology: applications in the environmental sciences, Kluwer Academic Publishers, Boston, 2013.

Díaz, S. C., Therrell, M. D., Stahle, D. W., and Cleaveland, M. K.: Chihuahua (Mexico) winter-spring precipitation reconstructed from tree-rings, 1647-1992, Clim. Res., 22, 237-244, https://doi:10.3354/cr022237, 2002.

Duan, J., Wang, L., Li, L., and Sun, Y.: Tree-ring-inferred glacier mass balance variation in southeastern Tibetan Plateau and its linkage with climate variability, Clim. Past., 9, 2451-2458, https://doi.org/10.5194/cp-9-2451-2013, 2013.

Fritts, H.: Tree rings and climate, Academic Press, London, 1976.

Gao, Z. H., Zhang, H. L., Chen, F., Satylkanov, R., Ermenbaev, B., Bakhtiyorov, Z., Zhang, R. B., Yu, S. L., Yue, W. P., Zhao, X. E.: Tree-ring based streamflow reconstruction of the Chu River in Kyrgyzstan over the past 407 years, Quaternary Sciences, 42, 288-301, https://doi.org/10.11928/j.issn.1001-7410.2022.01.23, 2022.

Guo, H., Bao, A. M., Chen, T., Zheng, G. X., Wang, Y. Q., Jiang, L. L., and De Maeyer, P.: Assessment of CMIP6 in simulating precipitation over arid Central Asia, Atmos Res, 252, https://doi.org/10.1016/j.atmosres.2021.105451, 2021.

Hagg, W. J., Braun, L. N., Uvarov, V. N., and Makarevich, K. G.: A comparison of three methods of mass-balance determination in the Tuyuksu glacier region, Tien Shan, Central Asia, J Glaciol, 50, 505-510, https://doi.org/10.3189/172756504781829783, 2017.

Hao, H. Q., Hao, Y. H., Liu, Y., Yeh, T. C. J., Zhang, M., Wang, Q., and Fan, Y. H.: Anomaly of glacier mass balance in different vertical zones and responses to climate modes: Urumqi Glacier No. 1, China, Clim Dynam, https://doi.org/10.1007/s00382-022-06318-w, 2022.

Harris, I., Osborn, T. J., Jones, P., and Lister, D.: Version 4 of the CRU TS monthly high-resolution gridded multivariate climate dataset, Sci. Data., 7, 109, https://doi.org/10.6084/m9.figshare.11980500, 2020.

Holmes, R. L.: Computer-assisted quality control in tree-ring dating and measurement, Tree-Ring. Bulletin., 43, 69-78, 1983.

Huss, M. and Hock, R.: Global-scale hydrological response to future glacier mass loss, Nat Clim Change, 8, 135-140, https://doi.org/10.1038/s41558-017-0049-x, 2018.

Jonaitis, J. A., Perry, L. B., Soulé, P. T., Thaxton, C., Andrade-Flores, M. F., Vargas, T. I., and Ticona, L.: Spatiotemporal patterns of ENSO-precipitation relationships in the tropical Andes of southern Peru and Bolivia, Int. J. Climatol., 41, 4061-4076, https://doi.org/10.1002/joc.7058, 2021.

Kang, J., Jiang, S. W., Tardif, J. C., Liang, H. X., Zhang, S. K., Li, J. Y., Yu, B. Y., Bergeron, Y., Rossi, S., Wang, Z., Zhou, P., and Huang, J. G.: Radial growth responses of two dominant conifers to climate in the Altai Mountains, Central Asia, Agr. Forest. Meteorol., 298-299,

https://doi.org/10.5194/hess-2022-329
Preprint. Discussion started: 19 September 2022

https://doi.org/10.1016/j.agrformet.2020.108297, 2021.

Kononov, Y. M., Ananicheva, M. D., and Willis, I. C.: High-resolution reconstruction of Polar Ural glacier mass balance for the last millennium, Ann Glaciol, 42, 163-170, https://doi.org/10.3189/172756405781812709, 2005.

Lan, J. H., Xu, H., Sheng, E. G., Yu, K. K., Wu, H. X, Zhou, K. G., Yan, D. N, Ye, Y. D, and Wang, T. L.: Climate changes reconstructed from a glacial lake in High Central Asia over the past two millennia, Quatern Int, 487, 43-53, https://doi.org/10.1016/j.quaint.2017.10.035, 2018.

Lan, J. H., Wang, T. L., Dong, J. B, Kang, S. G., Cheng, P., Zhou, K. E., Liu, X. X., Wang, Y. Q., and Ma, L.: The influence of ice sheet and solar insolation on Holocene moisture evolution in northern Central Asia, Earth-Sci. Rev., https://doi.org/10.1016/j.earscirev.2021.103645, 2021.

Larocque, S. J. and Smith, D. J.: 'Little Ice Age' proxy glacier mass balance records reconstructed from tree rings in the Mt Waddington area, British Columbia Coast Mountains, Canada, Holocene., 15, 748-757, https://doi.org/10.1191/0959683605hl848rp, 2005.

Li, J., Xie, S. P., Cook, E. R., Huang, G., D'Arrigo, R., Liu, F., Ma, J., and Zheng, X. T.: Interdecadal modulation of El Niño amplitude during the past millennium, Nat Clim Change, 1, 114-118, https://doi.org/10.1038/nclimate1086, 2011.

Li, Y., Tao, H., Su, B. D., Kundzewicz, Z. W., and Jiang, T.: Impacts of 1.5 °C and 2 °C global warming on winter snow depth in Central Asia, Sci. Total. Environ., 651, 2866-2873, https://doi.org/10.1016/j.scitotenv.2018.10.126, 2019.

Li, Z., Fang, G. H., Chen, Y. N., Duan, W. L., and Mukanov, Y.: Agricultural water demands in Central Asia under 1.5 °C and 2.0 °C global warming, Agr. Water. Manage., 231, https://doi.org/10.1016/j.agwat.2020.106020, 2020.

Linderholm, H. W., Jansson, P., and Chen, D.: A high-resolution reconstruction of Storglaciären mass balance back to 1780/81 using tree-ring data and circulation indices, Quatern. Res., 67, 12-20, https://doi.org/10.1016/j.yqres.2006.08.005, 2017.

Liu, L., Jiang, L. M., Wang, H. S., Ding, X. L., and Xu, H. Z.: Estimation of glacier mass loss and its contribution to river runoff in the source region of the Yangtze River during 2000-2018, J. Hydrol., 589, https://doi.org/10.1016/j.jhydrol.2020.125207, 2020.

Liu, Y., Wang, C. Y., Hao, W. J., Song, H. M., Cai, Q. F., Tian, H., Sun, B., and Linderholm, H. W.: Tree-ring-based annual precipitation reconstruction in Kalaqin, Inner Mongolia for the last 238 years,

https://doi.org/10.5194/hess-2022-329
Preprint. Discussion started: 19 September 2022

Hydrology and Earth System Sciences
Discussions

Chinese. Sci. Bull., 56, 2995-3002, https://doi.org/10.1007/s11434-011-4706-6, 2011.

Managave, S., Shimla, P., Yadav, R. R., Ramesh, R., and Balakrishnan, S.: Contrasting Centennial-Scale Climate Variability in High Mountain Asia Revealed by a Tree-Ring Oxygen Isotope Record From Lahaul-Spiti, Geophys. Res. Lett., 4, 47, https://doi.org/10.1029/2019GL086170, 2020.

Mann, M. E. and Lees, J. M.: Robust estimation of background noise and signal detection in climatic time series, Climatic. Change., 33, 409-445, https://doi.org/10.1007/BF00142586, 1996.

Marcinkowski, K.: Reconstructing mass balance of South Cascade Glacier using tree-ring records, 2012.

Mariotti, A.: How ENSO impacts precipitation in southwest central Asia, Geophys. Res. Lett., 34, https://doi.org/10.1029/2007GL030078, 2007.

Michaelsen, J.: Cross-Validation in Statistical Climate Forecast Models, J. Appl. Meteorol. Clim., 26, 1589-1600, https://doi.org/10.1175/1520-0450(1987)026<1589:CVISCF>2.0.CO;2, 1987.

Munia, H., Guillaume, J. H. A., Mirumachi, N., Porkka, M., Wada, Y., and Kummu, M.: Water stress in global transboundary river basins: significance of upstream water use on downstream stress, Environ Res Lett, 11, https://doi.org/10.1088/1748-9326/11/1/014002, 2016.

Shean, D. E., Bhushan, S., Montesano, P., Rounce, D. R., Arendt, A., and Osmanoglu, B.: A Systematic, Regional Assessment of High Mountain Asia Glacier Mass Balance, Front. Earth. Sc-Switz., 7, https://doi.org/10.3389/feart.2019.00363, 2020.

Shekhar, M., Bhardwaj, A., Singh, S., Ranhotra, P. S., Bhattacharyya, A., Pal, A. K., Roy, I., Martin-Torres, F. J., and Zorzano, M. P.: Himalayan glaciers experienced significant mass loss during later phases of little ice age, Sci. Rep-UK., 7, 10305, https://doi.org/10.1038/s41598-017-09212-2, 2017.

Singh, N., Shekhar, M., Singh, J., Gupta, A. K., Bräuning, A., Mayr, C., and Singhal, M.: Central Himalayan tree-ring isotopes reveal increasing regional heterogeneity and enhancement in ice mass loss since the 1960s, The. Cryosphere., 15, 95-112, https://doi.org/10.5194/tc-15-95-2021, 2021.

Smith, T. M. and Reynolds, R. W.: Extended reconstruction of global sea surface temperatures based on COADS data (1854–1997), J. Climate., 16, 1495-1510, https://doi.org/10.1175/1520-0442(2003)016<1495:EROGSS>2.0.CO;2, 2003.

Trouet, V., Esper, J., Graham, N. E., Baker, A., Scourse, J. D., and Frank, D. C. J.: Persistent positive North Atlantic Oscillation mode dominated the medieval climate anomaly, Science., 324, 78-80, https://doi.org/ 10.1126/science.1166349, 2009.

Vautard, R., Yiou, P., and Ghil, M.: Singular-spectrum analysis: A toolkit for short, noisy chaotic signals,

https://doi.org/10.5194/hess-2022-329
Preprint. Discussion started: 19 September 2022

Hydrology and Earth System Sciences
Open Access
EGU
Discussions

58, 95-126, https://doi.org/10.1016/0167-2789(92)90103-T, 1992.

Watson, E. and Luckman, B. H.: Tree-ring-based mass-balance estimates for the past 300 years at Peyto Glacier, Alberta, Canada, Quaternary. Res., 62, 9-18, https://doi.org/10.1016/j.yqres.2004.04.007, 2017.

Wigley, T. M. L., Briffa, K. R., and Jones, P. D.: On the Average Value of Correlated Time-Series, with Applications in Dendroclimatology and Hydrometeorology, J. Appl. Meteorol. Clim., 23, 201-213, https://doi.org/10.1175/1520-0450(1984)023<0201:OTAVOC>2.0.CO;2, 1984.

Wood, L. J., Smith, D. J., and Demuth, M. N.: Extending the Place Glacier mass-balance record to AD 1585, using tree rings and wood density, Quatern. Res., 76, 305-313, https://doi.org/10.1016/j.yqres.2011.07.003, 2011.

Xu, M., Kang, S. C., Wu, H., and Yuan, X.: Detection of spatio-temporal variability of air temperature and precipitation based on long-term meteorological station observations over Tianshan Mountains, Central Asia, Atmos. Res., 203, 141-163, https://doi.org/10.1016/j.atmosres.2017.12.007, 2018.

Yang, T., Li, Q., Chen, X., Hamdi, R., De Maeyer, P., and Li, L.: Variation of Snow Mass in a Regional Climate Model Downscaling Simulation Covering the Tianshan Mountains, Central Asia, J Geophys Res-Atmos, https://doi.org/10.1029/2020JD034183, 2021.

Yuan, Y. J., Shao, X. M., Wei, W. S., Yu, S. L., Gong, Y., and Trouet, V.: The Potential to Reconstruct Manasi River Streamflow in the Northern Tien Shan Mountains (NW China), Tree-Ring Res, 63, 81-93, https://doi.org/10.3959/1536-1098-63.2.81, 2007.

Yuan, Y. J., Wei, W. S., Chen, F., Yu, S. L., and Gong, Y.: Tree-ring reconstruction of annual total runoff for the Urumqi River on the northern slope of Tien Shan Mountains, Quaternary Sciences, 33, 501-510, https://doi.org/10.3969/j.issn.1001-7410.2013.03.10, 2013.

Zhang, H. L., He, Q., Chen, F., Chontoev, D., Satylkanov, R., Ermenbaev, B., and Chen, Y. P.: August-September Runoff Variation in the Kara Darya River Determined from Juniper (*Juniperus turkestanica*) Tree Rings in the Pamirs-Alai Mountains, Kyrgyzstan, Back to 1411 CE, Acta. Geol. Sin-Engl., 94, 682-689, https://doi.org/10.1111/1755-6724.14533, 2020.

Zhang, H. L., Shang, H. M., Chen, F., Chen, Y. P., Yu, S. L., and Zhang, T. W.: A 422-Year Reconstruction of the Kaiken River Streamflow, Xinjiang, Northwest China, Atmosphere, 11, https://doi.org/10.3390/atmos11101100, 2020.

Zhang, M., Chen, Y. N., Shen, Y. J., and Li, B. F.: Tracking climate change in Central Asia through temperature and precipitation extremes, J. Geogr. Sci., 29, 3-28, https://doi.org/10.1007/s11442-019-1581-6, 2019.

Zhang, R. B, Shang, H. M, Yu, S. L, He, Q., Yuan, Y. J, Bolatov, K., and Mambetov, B. T.: Tree-ring-based precipitation reconstruction in southern Kazakhstan, reveals drought variability since A.D. 1770, Int J Climatol, 37, 741-750, https://doi.org/10.1002/joc.4736, 2017.

Zhang, R. B., Wei, W. S., Shang, H. M., Yu, S. L., Gou, X. H, Qin, L., Bolatov, K., and Mambetov, B. T.: A tree ring-based record of annual mass balance changes for the TS.Tuyuksuyskiy Glacier and its linkages to climate change in the Tianshan Mountains, Quaternary. Sci. Rev., 205, 10-21, https://doi.org/10.1016/j.quascirev.2018.11.028.

Zhang, R. B., Zhang, T. W., Kelgenbayev, N., He, Q., Maisupova, B., Mambetov, B. T., Chen, F., Dosmanbetov, D., Shang, H. M., Yu, S. L., and Yuan, Y. J.: A 189-year tree-ring record of drought for the Dzungarian Alatau, arid Central Asia, Quaternary. Sci. Rev., 148, 305-314, https://doi.org/10.1016/j.jseaes.2017.05.003, 2017.

Zhang, T. W, Lu, B., Zhang, R. B, Diushen, M., Rysbek, S., Bakytbek, E., Chen, F., Yu, S. L, Jiang, S. X, and Zhang, H. L: A 256-year-long precipitation reconstruction for northern Kyrgyzstan based on tree-ring width, Int J Climatol, 40, 1477-1491, https://doi.org/10.1002/joc.6280, 2019.

Zhang, T. W., Zhang, R. B., Yuan, Y. J., Gao, Y. Q., Wei, W. S., Diushen, M., He, Q., Shang, H. M., and Wang, J.: Reconstructed precipitation on a centennial timescale from tree rings in the western Tien Shan Mountains, Central Asia, Quatern. Int., 358, 58-67, https://doi.org/10.1016/j.quaint.2014.10.054, 2015.

Zhu, M., Yang, W., Yao, T., Tian, L., Thompson, L. G., and Zhao, H.: The Influence of Key Climate Variables on Mass Balance of Naimona'nyi Glacier on a North‐Facing Slope in the Western Himalayas, J Geophys Res-Atmos, 126, https://doi.org/10.1029/2020JD033956, 2021.